

# Harmonic distortion in microwave photonic filters

Manuel Rius, José Mora,\* Mario Bolea, and José Capmany

ITEAM Research Institute, Universidad Politécnica de Valencia, C/ Camino de Vera, s/n 46022 Valencia, Spain

\*jmalmer@upv.es

**Abstract:** We present a theoretical and experimental analysis of nonlinear microwave photonic filters. Far from the conventional condition of low modulation index commonly used to neglect high-order terms, we have analyzed the harmonic distortion involved in microwave photonic structures with periodic and non-periodic frequency responses. We show that it is possible to design microwave photonic filters with reduced harmonic distortion and high linearity even under large signal operation.

©2012 Optical Society of America

**OCIS codes:** (060.0060) Fiber optics and optical communications; (060.5625) Radio frequency photonics.

---

## References and links

1. J. Capmany and D. Novak, "Microwave photonics combines two worlds," *Nat. Photonics* **1**(6), 319–330 (2007).
2. J. Yao, "Microwave photonics," *J. Lightwave Technol.* **27**(3), 314–335 (2009).
3. J. Capmany, B. Ortega, and D. Pastor, "A tutorial on Microwave Photonic Filters," *J. Lightwave Technol.* **24**(1), 201–229 (2006).
4. R. A. Minasian, K. E. Alameb, and E. H. W. Chan, "Photonics-based interference mitigation," *IEEE Trans. Microw. Theory Tech.* **49**(10), 1894–1899 (2001).
5. M. Bolea, J. Mora, B. Ortega, and J. Capmany, "Photonic arbitrary waveform generation applicable to multiband UWB communications," *Opt. Express* **18**(25), 26259–26267 (2010).
6. J. Dai, K. Xu, X. Sun, Y. Li, J. Niu, Q. Lv, J. Wu, X. Hong, and J. Lin, "Instantaneous frequency measurement system with tunable measurements range utilizing fiber-based incoherent microwave photonic filters," in *Proc. Microwave Photonics 2010 MWP '10. Int. Topical Meeting on, Montreal*, 1–4 (2010).
7. J. Capmany, D. Pastor, and B. Ortega, "New and flexible fiber-optic delay line filters using chirped Bragg gratings and laser arrays," *IEEE Trans. Microw. Theory Tech.* **47**(7), 1321–1326 (1999).
8. J. Mora, B. Ortega, J. Capmany, J. Cruz, M. Andres, D. Pastor, and S. Sales, "Automatic tunable and reconfigurable fiberoptic microwave filters based on a broadband optical source sliced by uniform fiber Bragg gratings," *Opt. Express* **10**(22), 1291–1298 (2002).
9. J. Capmany, J. Mora, B. Ortega, and D. Pastor, "Microwave photonic filters using low-cost sources featuring tunability, reconfigurability and negative coefficients," *Opt. Express* **13**(5), 1412–1417 (2005).
10. T. X. H. Huang, X. Yi, and R. A. Minasian, "Single passband microwave photonic filter using continuous-time impulse response," *Opt. Express* **19**(7), 6231–6242 (2011).
11. Y. Dai and J. Yao, "Nonuniformly-spaced photonic microwave delayline filter," *Opt. Express* **16**(7), 4713–4718 (2008).
12. J. Mora, B. Ortega, A. Díez, J. L. Cruz, M. V. Andrés, J. Capmany, and D. Pastor, "Photonic microwave tunable single-bandpass filter based on a Mach-Zehnder Interferometer," *J. Lightwave Technol.* **24**(7), 2500–2509 (2006).
13. D. Marcuse, "Pulse distortion in single-mode fibers," *Appl. Opt.* **19**(10), 1653–1660 (1980).

---

## 1. Introduction

Microwave photonics (MWP) is defined as a research area which combines both microwave and optical fields covering a large number of topics including photonic generation, processing, control and distribution of microwave and millimeter-wave signals. MWP has been the subject of a great interest in last years as it enables functionalities such as fast tunability and reconfigurability that conventional electronic methods cannot achieve. Indeed, photonics technology brings the inherent advantages of operating in the optical domain: low loss, light weight, high bandwidth and immunity to electromagnetic interference (EMI). Additionally, MWP systems can be directly incorporated into Radio-over-fiber (RoF)

networks where the signals can be processed directly in the optical domain without the need of additional electrical/optical (E/O) and optical/electrical (O/E) conversions [1, 2].

In this context, MWP filters are considered a key element in the processing and control of radiofrequency (RF) signals in the optical domain, being suitable for a great number of applications since they are free from bandwidth constraint [3]. As an example, RoF systems require channel rejection and channel selection [4]. Also, alternative applications related to arbitrary waveform generation [5] and the measurement of instantaneous frequency for modern radar [6] have been demonstrated by photonic filtering.

Different proposals have been reported in the literature to implement MWP filters. One of the most versatile is that based on an array of optical lasers and a linear chirped fiber grating to introduce the different delays between the optical taps [7]. In order to avoid the extra cost derived from the use of multiple sources, the slicing of a broadband source performed by a set of fiber Bragg gratings [8] and an arrayed waveguide grating (AWG) [9] have been proposed. In either case, the implemented filters present a periodic spectral response with multiple passbands. However, a single bandpass filtering response can be achieved with structures based on phase-to-intensity conversion [10] and continuous time impulse response [11, 12]. Most of the reported work on MWP filters focus exclusively on their linear behavior, assuming small signal operation, but it is a fact, as with any filtered microwave photonic link, that nonlinearities are to be expected in the form of harmonic contributions to the filter overall transfer function. These contributions are of special interest when the modulating signal cannot be considered of small amplitude.

In this work, we present a theoretical evaluation of the high order distortion involved in MWP filters operating under large signal regime. Also, we experimentally show the harmonic distortion of two different microwave photonic filtering structures which are based on the slicing of a broadband source (BBS) combined with a dispersive single mode fiber (SMF) link. We consider a discrete slicing achieved by a structure of AWGs obtaining a periodical electrical response [9] and a quasi-continuous slicing by means of a Mach-Zehnder Interferometer (MZI) yielding a non-periodic response [12]. The experimental and theoretical analysis of these electrical responses yield an excellent agreement revealing the interest of considering this harmonic distortion model on the design of advanced microwave photonic filters to exploit the MWP benefits.

## 2. Theoretical analysis of harmonic distortion involved in MWP filters

In Fig. 1, we represent the scheme which is used to explain the theoretical analysis to describe the harmonic distortion involved in microwave photonic filtering. Note that this discussion can be extended to alternative configurations previously reported in the literature without loss of generality.

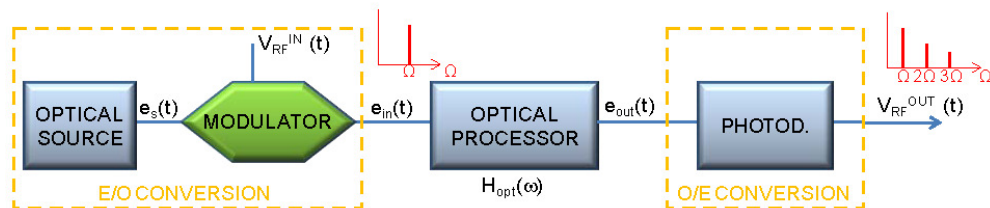


Fig. 1. Scheme of a microwave photonic filter when harmonic distortion is considered.

Following Fig. 1, an optical source which is defined through the optical field  $e_s(t)$  and the corresponding optical spectrum  $E_s(\omega)$  is modulated by means of an electrical to optical (E/O) conversion. For it, we can employ an external modulator since high frequency operation range is considered. Therefore, the optical field at the output of the modulator can be written as:

$$e_{IN}(t) = \frac{1}{\sqrt{2\pi}} \sum_{n=-\infty}^{+\infty} \left\{ \int_{-\infty}^{+\infty} s_n(V_o) \cdot E_s(\omega) \cdot e^{j(\omega+n\Omega)t} \cdot d\omega \right\} \quad (1)$$

Where  $s_n$  represents the modulation coefficient for each harmonic of n-order when an input RF signal  $V_{RF}^{IN}(t) = V_o \cdot \cos(\Omega t)$  is applied to the electrooptical modulator (EOM).

From Eq. (1), we can observe that the E/O conversion from the input RF signal  $V_{RF}^{IN}(t)$  to the input optical field  $e_{IN}(t)$  in the optical subsystem is a nonlinear process. The signal linearity is only guaranteed between the input and output optical fields, being established by means of the optical optical field transfer function  $H_{opt}(\omega)$ . Therefore, the output optical field  $e_{OUT}(t)$  is given by [13]:

$$e_{OUT}(t) = \frac{1}{\sqrt{2\pi}} \sum_{n=-\infty}^{+\infty} \left\{ \int_{-\infty}^{+\infty} s_n E_s(\omega) \cdot H_{opt}(\omega + n\Omega) e^{j(\omega+n\Omega)t} \cdot d\omega \right\} \quad (2)$$

Finally, the optical field  $e_{OUT}(t)$  is detected by means of a photodetector (PD) yielding as a result the output voltage  $V_{RF}^{OUT}(t)$  which is given by:

$$V_{RF}^{OUT}(t) = \Re \left\langle |e_{OUT}(t)|^2 \right\rangle \cdot Z_o \quad (3)$$

Here  $\Re$  is the detector responsivity and  $Z_o$  its impedance. The above expression shows as the output RF signal is nonlinearly related to the output optical field since the optical field to electrical current conversion upon detection is a nonlinear process. As known, linearity is only obtained under special operating conditions of low signal modulation. In any other case, a non linear relationship is expected to be found between the input and output RF signals. Therefore, we can define an electrical transfer function  $H_k^{RF}(\Omega)$  for each k-order term, which describes the harmonic distortion from the input RF signal  $V_{RF}^{IN}(t) = V_o \cdot \cos(\Omega t)$ :

$$V_{RF}^{OUT}(t) = \frac{V_o}{2} \sum_{k=-\infty}^{+\infty} H_k^{RF}(\Omega) \cdot e^{jk\Omega t} + c.c. \quad (4)$$

At this point, we consider that the optical processor consists on a dispersive element of length L with an optical field transfer function given by:

$$H_{opt}(\omega) = e^{-j\beta(\omega)L} \quad \text{with} \quad \beta(\omega) = \beta_o(\omega_o) + \beta_1(\omega - \omega_o) + \frac{1}{2}\beta_2(\omega - \omega_o)^2. \quad (5)$$

$\beta_o$  is the propagation constant at the central optical frequency  $\omega_o$ ,  $\beta_1$  is the group delay time and  $\beta_2$  is the first order dispersion at the same optical frequency.

Substituting Eq. (5) into Eq. (2), we can obtain the output voltage from Eq. (3) by taking into account that the optical source is described as a non-stationary process with a loss of generality [13]. Finally, comparing the obtained results with the description of Eq. (4), we can identify the electrical transfer function  $H_k^{RF}(\Omega)$  for each k-order harmonic, which is given by:

$$H_k^{RF}(\Omega) = \frac{\Re P_o \cdot Z_o}{\pi V_o} \cdot e^{j\beta_1 L(k\Omega)} \underbrace{\sum_{n=-\infty}^{+\infty} s_n s_{n-k}^* e^{-j\frac{1}{2}\beta_2 L(k-2n)\Omega^2}}_{CSE} \cdot \frac{\int_{-\infty}^{+\infty} |E(\omega)|^2 \cdot e^{j\beta_2 L(\omega - \omega_o)(k\Omega)} \cdot d\omega}{\int_{-\infty}^{+\infty} |E(\omega)|^2 \cdot d\omega} \quad (6)$$

The first factor inside the sum in Eq. (6) takes into account the E/O and O/E conversion efficiency. The second factor corresponds to the conventional electrical response of the  $k$ -harmonic when a monochromatic optical source centered at the optical frequency  $\omega_0$  is considered and is related to the carrier suppression effect (CSE). The key term of the analysis corresponds to the last factor which is related to the filtering effects of the microwave photonic structure which depends, in turn, on the optical source and the optical processor through the optical power spectrum and the dispersion, respectively. Therefore, the theoretical analysis reveals that the electrical transfer function of each harmonic also suffers a microwave photonic filtering effect with a scale factor given by that of the  $k$ -order harmonic.

### 3. Experimental Results and Discussion

With the aim of evaluating the nonlinear response of different microwave photonic filters, an experimental setup was implemented according to Fig. 2 since it permits to analyze different electrical responses considering two different optical sources and an amplitude modulator.

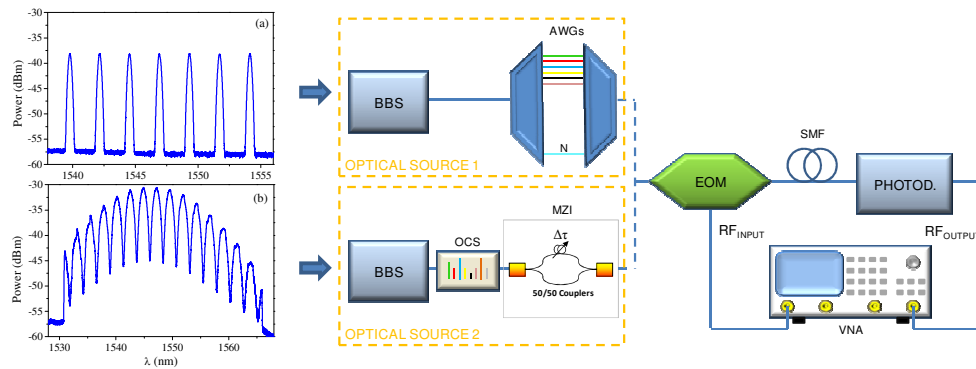


Fig. 2. Experimental setup for measurements of the electrical transfer function in microwave photonic filters with harmonic distortion. Inset (a) corresponds to uniform profile sliced combining AWGs and inset (b) to gaussian profile sliced by MZI.

Both filters are designed to give a frequency resonance around 4.56 GHz using a 5 km dispersive fiber link by selecting a uniform profile and a gaussian profile with discrete optical samples combining array waveguides gratings (AWGs) and continuous samples by slicing a broadband source with an interferometric structure (MZI), respectively. A 48-channel optical channel selector (OCS) is employed with a 0.8 nm channel width. The attenuation of each channel can be independently controlled to obtain the gaussian distribution. Insets of Fig. 2 plot the corresponding optical source power spectrum. For both cases, an 80 nm ASE source is employed as broadband source (BBS). Initially, a BBS can introduce a large intensity noise but a balanced differential photodetection can minimize this restriction [5].

For a given optical source, the optical signal is amplitude modulated by an external electrooptic modulator (EOM), in which the RF-signal of frequency  $\Omega = 2\pi f$  is generated by a vector network analyzer (VNA) with an RF power of 20 dBm. The modulated signal is driven to a 5 km of fiber link which acts as an optical processor. Finally, the output optical signal is detected and the electrical transfer function of the filter is measured in the VNA.

Figure 3 plots the photodetected RF power for fundamental tone  $P_{RF}(\Omega)$ , the second harmonic  $P_{RF}(2\Omega)$  and the third harmonic  $P_{RF}(3\Omega)$  for both microwave photonic filters subject to consideration. The left column of Fig. 3 plots measurements of a filter defined by an uniform optical source with 7 equalized discrete samples coming from the AWG structure [9]. As observed, the electrical response has a periodic behaviour and the electrical transfer function of each harmonic is scaled according to the corresponding  $k$ -order factor. If the first resonance is considered as a representative electrical subcarrier ( $f_0 = 4.56$  GHz), we obtain

for the power levels of the second and third harmonic values which are respectively 18 and 24 dB below the  $-54.5$  dBm RF power measured for the fundamental tone. In addition, we observe that the electrical responses decrease due to CSE (dotted line), which is generated by the beating of the harmonic terms along the dispersive fiber and is contained in the second term of Eq. (6). Note that theoretical predictions (dashed lines) show an excellent agreement with experimental results (solid lines).

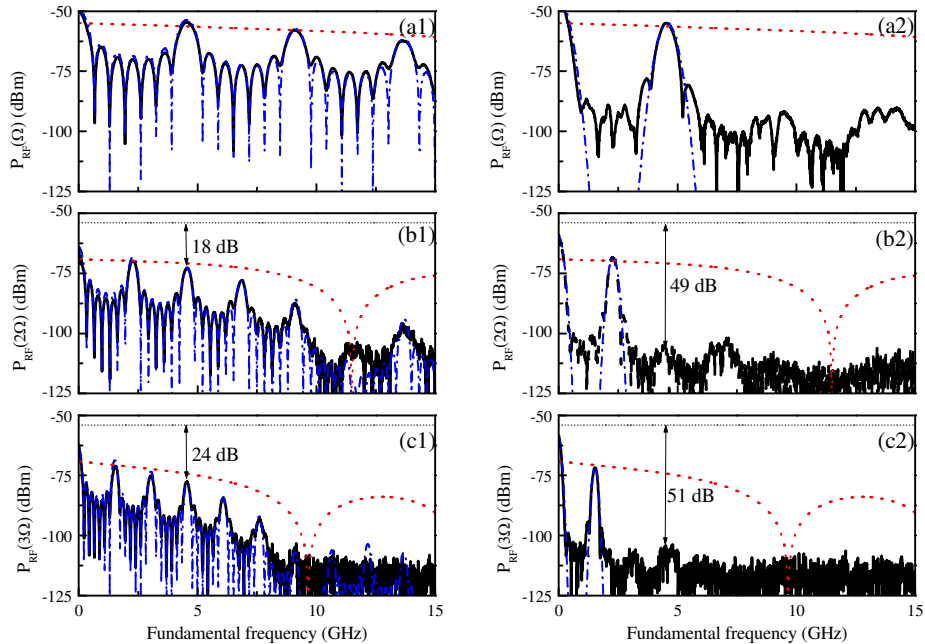


Fig. 3. Experimental (solid line) and theoretical (dashed line) RF power of (a) fundamental tone, (b) second harmonic and (c) third harmonic for (left column) AWGs slicing and (right column) MZI slicing. Dotted line represents theoretical CSE for (a) fundamental tone, (b) second harmonic and (c) third harmonic.

The measurements corresponding to the second microwave photonic filter are illustrated in right column of Fig. 3. In this case, note that the fundamental electrical transfer function has a single bandpass centered at the designed frequency  $f_o = 4.56$  GHz since the optical source has a gaussian profile sliced with a sinusoidal pattern [12]. Note that this filter is more selective as compared to the previous case and, therefore, it is expected that the nonlinear electrical responses have a different behaviour. Indeed, Fig. 3(b2) and 3(c2) show that the corresponding RF powers of the second and third harmonics also have a single bandpass characteristic with resonance maxima also scaled by the  $k$ -order coefficient. A higher level of harmonic suppression is achieved with 49 dB and 51 dB for the electrical subcarrier of 4.56 GHz. Clearly, this filter achieves higher reduction of high-order harmonics than in previous case (discrete sampled source). Again, the theoretical results show an excellent agreement with the experimental electrical response for each  $k$ -order according to Eq. (6)

Finally, we have performed a comparison of the harmonic distortion measurements of both configurations as function of the RF input power. The objective is to analyze their immunity to nonlinear effects as related to the input modulating RF signal. Figure 4 plots the photodetected RF power of the first harmonic  $P_{RF}(\Omega)$ , the second harmonic  $P_{RF}(2\Omega)$  and the third harmonic  $P_{RF}(3\Omega)$  as a function of RF input power for the fundamental tone  $f_o = 4.56$  GHz which corresponds to the first resonance of both microwave photonics filters considered. Measurements obtained with AWG slicing in Fig. 4(a) have a similar behaviour to the

response obtained when a laser array is used as an optical source due to periodicity of its electrical transfer function. Indeed, the nonlinearities of the filtering structure come exclusively from the E/O and O/E conversion processes. However, Fig. 4(b) shows measurements corresponding to the case when the broadband source is continuously sliced by means of a MZI. A clear difference with respect to previous filter can now be observed. In this second case, the RF power of second and third harmonic is reduced considerably due to the fact that its electrical transfer function has a single bandpass. We have measured a spurious-free dynamic range (SFDR) of  $40 \text{ dB}\cdot\text{Hz}^{1/2}$  for the AWG slicing filter meanwhile with MZI slicing filter we obtain a SFDR value of  $60 \text{ dB}\cdot\text{Hz}^{1/2}$ , respectively. This means that using the MZI slicing filter configuration is possible to achieve a much higher harmonic suppression in the electrical transfer function. In all cases, a good agreement is found between the theoretical and experimental results where average noise signal level is around  $-145 \text{ dBm/Hz}$ . In our case, SFDR is defined as the carrier-to-noise ratio when the noise floor ( $P_{\text{noise}}$ ) in the signal bandwidth equals to the power of a second order intermodulation product ( $IP_2$ ),  $\text{SFDR}(\text{dB}\cdot\text{Hz}^{1/2}) = 1/2 \cdot (IP_2 - P_{\text{noise}})$ .

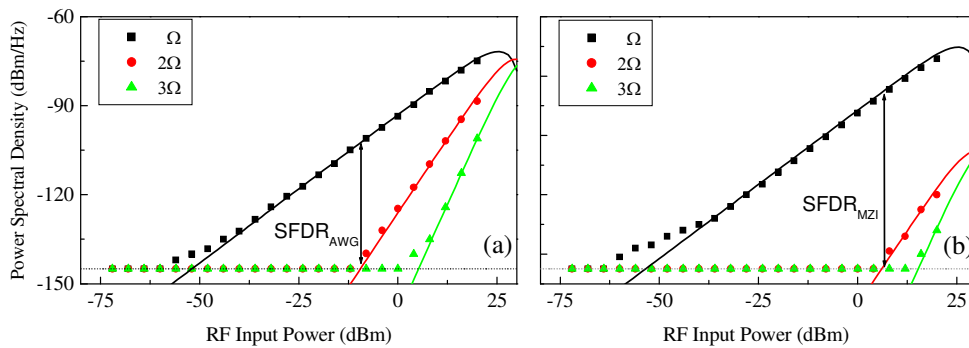


Fig. 4. Experimental (dotted line) and theoretical (solid line) RF power of (■) fundamental tone, (●) second and (▲) third harmonic for (a) AWGs and (b) MZI slicing as a function of RF input power.

#### 4. Conclusion

We have presented a theoretical evaluation and an experimental demonstration of the impact of harmonic distortion in microwave photonic filters. We have compared different MWP structures in order to show the impact of considering a laser signal operation. Indeed, we have demonstrated that the design of MWP filters taking into account the harmonic distortion permits to achieve additional filtering properties as the linearization of the system. Therefore, the interest to consider this harmonic distortion model on the design of advanced microwave photonic filters is demonstrated.

#### Acknowledgments

The authors wish to acknowledge the financial support given by the Research Excellency Award Program GVA PROMETEO 2008/09 and the FEDER Program “Instrumentación Avanzada para Comunicaciones Ópticas” with reference UPVOV08-3E-008.